# Development of cavity and microstrip resonators for electron spin resonance experiments

*A thesis submitted in partial fulfilment of the requirements for the award of the degree of*

Master of Science by Research

by

**Sandeep Tammu**

13MR002

under

**Dr. Chiranjib Mitra**

to the

**Department of Physical Sciences**


INDIAN INSTITUTE OF SCIENCE EDUCATION AND RESEARCH KOLKATA

[April, 2015]

# Declaration of the student on Academic Integrity and Copyright

I hereby declare that this thesis is my own work and, to the best of my knowledge, it contains no materials previously published or written by any other person, or substantial proportions of material which have been accepted for the award of any other degree or diploma at IISER Kolkata or any other educational institution, except where due acknowledgement is made in the thesis. I certify that all copyrighted material incorporated into this thesis is in compliance with the Indian Copyright (Amendment) Act, 2012 and that I have received written permission from the copyright owners for my use of their work, which is beyond the scope of the law. I agree to indemnify and save harmless IISER Kolkata from any and all claims that may be asserted or that may arise from any copyright violation.

Signed: _____

Date: _____

# Certificate of the Supervisor

This is to certify that the Masters' thesis entitled "Development of cavity and microstrip resonators for electron spin resonance experiments" represents original research work to the best of our knowledge except where due acknowledgements are made. Sandeep is the sole author of the thesis and it contains no material that has been submitted previously, in whole or in part, for the award of any other academic degree or diploma, either in IISER-Kolkata or in any other institute.

May, 2015
IISER Kolkata

Chiranjib Mitra

UNIVERSITY NAME (IISER KOLKATA)

# *Abstract*

Dr. Chiranjib Mitra
Department of Physical Sciences

Master of Science by Research

**Development of cavity and microstrip resonators for electron spin resonance experiments**

by Sandeep Tammu

Electron spin resonance is used as a spectroscopic tool for studying magnetic systems in many areas of science. Generally, cavity resonators are used to generate the oscillating microwave field. There is a necessity for improving the performance of the existing resonators, as well as designing planar resonators in the X-band region of frequencies. This thesis work presents a cavity operating in transverse electric mode (TE011) and also a planar resonator operating at 11 GHz. The cavities showed good results in continuous EPR spectroscopy. Although proposed microstrip resonators did not perform as good as the reported designs, an improved design is suggested for the future. Planar resonators are advantageous in pulsed ESR and these microstrip resonators will be useful in spin-based quantum information processing.

# *Acknowledgements*

It is a pleasure to acknowledge my respect and gratitude for Dr. Chiranjib Mitra, my thesis supervisor, for not only providing me the opportunity to work on this fascinating problem but also for his sincere guidance and warm encouragement throughout the period of work.

I would like to thank graduate students Mr. Jit Sarkar, Mr. Sourabh Singh and Mr. Radhe Krishna Goapl, Mr. Tanmoy Chakraborthy and Mr. Harkirat Singh for their active support and advice. I would also like to thank Mr. Dipanjan Chaudhuri and Mr. Uditendu Mukhopadayay, masters students at IISER, Kolkata for their timely help.

I would like to express my sincere gratitude to Mr. Pavan from Rhode and Schwartz for his active help whenever I was struck.

Above all I would take this opportunity to thank my parents once again who have been my real sources of inspiration, strength and courage. As always, they have inspired me constantly to work hard and thrive for success....

# Contents

# List of Figures

*Dedicated to my parents...*

# Chapter 1

# Introduction and Motivation

## 1.1 Electron Paramsgnetic Resonance

Electron Paramagnetic resonance (EPR or ESR) is a spectroscopic tool used in many areas of science, engineering, chemistry, biology and physics for the study of magnetic samples. In this thesis, a traditional cavity operating in transverse electric mode is designed for doing EPR experiments. After successfully getting an EPR absorption spectrum in continuous mode, a microstrip resonator (MR) was designed having a resonant frequency in the X-band (8- 12 GHz). Unlike cavities, the propagation mode in MR is a transverse electromagnetic wave. Although the microstrip resonators did not show good performance when compared with cavities, an improved design has been proposed and simulated.

The conventional resonators for EPR are optimized for large samples (more than $1mm^3$). The sensitivity for the small samples, thin films and nano-magnets can be increased by using two parameters. As the sensitivity is directly proportional to quality factor(Q) and the filling factor of the cavity, one can increase either of them in increasing the sensitivity of the spin detection. For the cavities operating in TE mode, the main aim of the design is to have a higher quality factor. This will increase the spin sensitivity.

$$\eta = \frac{V_s}{V_c} \tag{1.1}$$

where $V_s$ is the volume of the sample

$V_c$ is the volume of cavity

On the other hand, for the microstrip resonators, although they have low Q-factor, the sample filling factor is high because the volume of the resonator is low. This will also

increase the spin sensitivity. Moreover, planar resonators can be easily simulated and fabricated using cheap lithographic methods. This provides a genuine advantage over cavity resonators because making 3-D structures is considerably difficult.

In addition to that, the planar resonators occupy lesser volume when compared to cavities, providing an easier way to do low temperature measurements. Strong magnetic field can be generated using very little microwave power, and very low dissipation. It has been well known that these microresonators will be useful in spin-based quantum information processing [1].

## 1.2 Origin of EPR

Every electron has a magnetic moment and spin quantum number $s = \frac{1}{2}$ , with magnetic components $m_s = +\frac{1}{2}$ and $m_s = -\frac{1}{2}$ . In the presence of an external magnetic field with strength $B_0$ , the electron's magnetic moment aligns itself either parallel ($m_s = -\frac{1}{2}$) or antiparallel ($m_s = +\frac{1}{2}$) to the field, each alignment having a specific energy due to the Zeeman effect :

$$E = m_s g_e \mu_B B_0 \tag{1.2}$$

where $g_e$ is the electron's so-called g-factor $g_e$ =2.0023 for the free electron $\mu_B$ is the Bohr magneton. Therefore, the separation between the lower and the upper state is $\Delta E = g_e \mu_B B_0$ for unpaired free electrons. This equation implies that the splitting of the energy levels is directly proportional to the magnetic field's strength, as shown in the diagram below [2].

We use a Vector network analyzer (VNA)[3] as a fixed microwave source which excites the electrons from lower energy levels. In addition to that, an external magnetic field is applied by using an electromagnet. In order for the transition to occur, the external field has to be swept in such a way that the energy separation will be matched with the microwave frequency. This leads to an absorption of energy in the energy spectrum, and can be measured in the vector network analyzer.

## 1.3 Definitions

### 1.3.1 Return Loss

Return loss is the amount of power lost because of the reflection in a transmission line. It is measured in dB [4] .

$$RL(dB) = -20log|\Gamma| \tag{1.3}$$

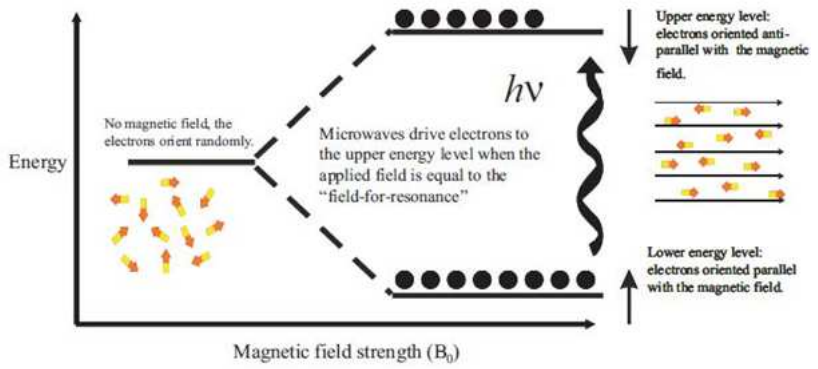


FIGURE 1.1: EPR: Zeeman effect

where Γ is the reflection coefficient. When the source and load impedances are known values, the reflection coefficient is given by

$$\Gamma = \frac{Z_{\mathrm{L}} - Z_{\mathrm{S}}}{Z_{\mathrm{L}} + Z_{\mathrm{S}}} \tag{1.4}$$

where $Z_L$ is the load impedance and $Z_S$ is the source impedance.

### 1.3.2 VSWR

Voltage standing wave ratio (VSWR) is a measure of amount of impedance matching in the network.

$$VSWR = \frac{1 + |\Gamma|}{1 - |\Gamma|} \tag{1.5}$$

where Γ is the reflection coefficient

When VSWR is 1, it indicates that the source is perfectly matched. In real world applications, a VSWR of 2:1 or just 2 is considered acceptable [5]. This table shows the return loss values for various VSWR.

| Return Loss(dB) | VSWR |
|---|---|
| 6dB | 3.009 |
| 10dB | 1.924 |
| 20dB | 1.222 |
| 25dB | 1.119 |
| 30dB | 1.063 |

# Chapter 2

# Cavity Resonators for Electron Spin Resonance

## 2.1 Microwave Cavities

Cavity is a metallic structure which can confine electromagnetic fields in the microwave region. As the electromagnetic field is confined inside the cavity, it has to satisfy certain boundary conditions depending upon the geometry of the cavity. The structure is generally hollow or filled with a dielectric material.

An ideal microwave cavity would have extremely low loss at its frequency of operation and cavities having quality factors upto $10^6$ were reported in the literature.

## 2.2 Theory of Microwave Cavities

At low frequencies, the behavior of circuit elements like Resistor is well-studied. An ideal resistor should not allow capacitive or inductive behavior. But, real resistors contain negligible inductance and capacitance. As the frequency is increased, these small frequencies ($\omega$L and $\frac{1}{\omega c}$) becomes important and one can not neglect these effects anymore. Hence, ordinary circuit elements are inefficient to transmit electromagnetic waves in GHz. range.

The behavior of a cylindrical cavity can be understood, when one thinks in terms of electric and magnetic fields produced when alternating current is applied to a parallel plate capacitor. Let an alternating voltage of frequency $\omega$ be applied to a parallel plate

FIGURE 2.1: A typical Cylindrical Cavity Resonator

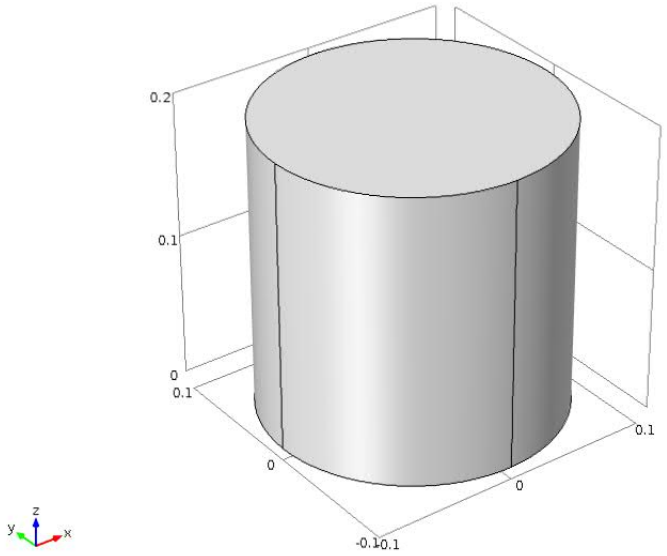


capacitor. The magnitude of electric field inside the capacitor can be taken as

$$E = E_0 \exp(i\omega t) \tag{2.1}$$

A change in electric field produces a magnetic field. Hence, the magnetic field is given by

$$B = \frac{i\omega r}{2c^2} E_0 \exp(i\omega t) \tag{2.2}$$

When there is a changing magnetic field, the electric field can not be uniform anymore. According to Faraday's law of electromagnetic induction, any time varying magnetic field will induce an electromotive force (emf) in a closed circuit. This induced emf is equivalent to a an electric field which is like the time derivative of the line integral of the electromagnetic field. Let the initial electric field be $E_1$ and the correction to the electric field be $E_2$ Total electric field

$$E = E_1 + E_2 \tag{2.3}$$

Let's calculate the value of $E_2$.

$$E_2(r) = \frac{\partial}{\partial t} \int B(r) dr \tag{2.4}$$

Using the above equation, we have

$$E_2(r) = -\frac{\omega^2 r^2}{2c^2} E_0 \exp i\omega t \tag{2.5}$$

The corrected electric field is

$$E = E_1 + E_2 = (1 - \frac{1}{4}\frac{\omega^2 r^2}{c^2})E_0 \exp(i\omega t) \tag{2.6}$$

Again, this new corrected electric field produces a magnetic filed. From Faraday's law, the new magnetic field corresponds to electric field and let the next correction to the electric field be $E_3$. In this way, the total electric field would be a series sum of the following terms.

$$E = E_1 + E_2 + E_3 + ..... = E_0 \exp(i\omega t)[1 - \frac{1}{(1!)^2}(\frac{\omega r}{2c})^2 + \frac{1}{2!^2}(\frac{\omega r}{2c}^4) - .....] \tag{2.7}$$

The above equation can be written as

$$E = E_0 exp(i\omega t) J_0(\frac{\omega r}{c}) \tag{2.8}$$

Where $J_0$ is the Bessel function of Zeroth order.

It can been seen that although appearance of Bessel Functions seems mysterious in the beginning, it follows from simple application of Maxwell's equations [6] .

FIGURE 2.2: Bessel Function of First Kind

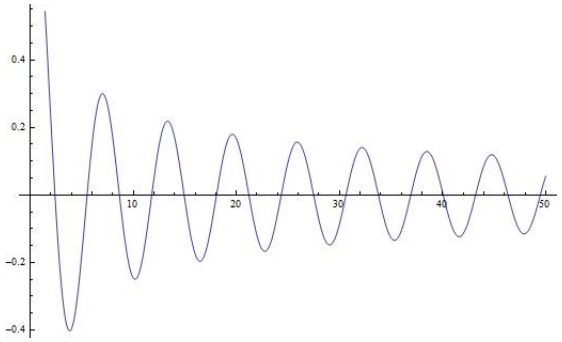


## 2.3 Cylindrical Cavity Resonators

A cylindrical cavity is formed by a section of circular waveguide by shorting at the both ends. When both the ends are closed, the fields have to satisfy additional boundary conditions.

The wave function in cylindrical cavity resonators should satisfy Maxwell's equations, subjected to same boundary conditions. Two types of modes can be observed in a cylindrical cavity.

FIGURE 2.3: Coordinates of a Cylindrical Cavity

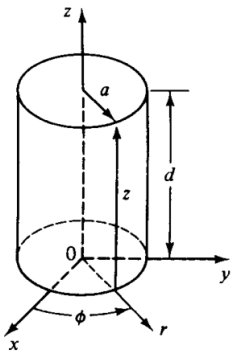


### 2.3.1 TE Modes

TE modes are characterized by no electric field component along the direction of propagation [7] . These can be achieved if

$$H_Z = H_{0z} J_n \left( \frac{X'_{np} r}{a} \right) cos(n\phi) sin \left( \frac{q\pi z}{d} \right) \tag{2.9}$$

where n=0,1,2,3...is the number of the periodicity in the $\phi$ direction

p=1,2,3...is the number of zeros of the field in the radial direction

q=1,2,3...is the number of half-waves in the axial direction

$J_n$ is the Bessel function of first kind

$H_{0Z}$ is the amplitude of the magnetic field

The wave number 'k' in TE Modes is given by

$$k^2 = \left( \frac{X'_{np} r}{a} \right)^2 + \left( \frac{q\pi}{d}^2 \right) \tag{2.10}$$

Substitution of $k^2 = \omega^2 \epsilon \mu$, the Resonant frequencies are given by

$$f_r = \frac{1}{2\pi\sqrt{\mu\epsilon}} \sqrt{\left( \frac{X'_{np}}{a}^2 \right) + \left( \frac{q\pi}{d} \right)^2} \tag{2.11}$$

### 2.3.2 TM Modes

TM modes are characterized by no magnetic field component along the direction of propagation [7]. These can be achieved if

$$E_z = E_{0z} J_n \left(\frac{X_{np} r}{a}\right) cos(n\phi) cos\left(\frac{q\pi z}{d}\right) \tag{2.12}$$

The wave number 'k' in TM Mode is given by the equation

$$k^2 = \left(\frac{X'_{np}}{a}^2\right) + \left(\frac{q\pi}{d}\right)^2 \tag{2.13}$$

By substituting 'k', the resonant frequency is given by

$$f_r = \frac{1}{2\pi\sqrt{\mu\epsilon}} \sqrt{\left(\frac{X_{np}}{a}^2\right) + \left(\frac{q\pi}{d}\right)^2} \tag{2.14}$$

## 2.4 Theoretical Resonant Frequencies of Cavities

For a cavity with height 18 mm and radius 18 mm, a MATLAB Program[1] is written to generate all the resonant frequencies. The results are tabulated in the figure.

| Mode | Theoretical Frequency(GHz) | Mode | Theoretical Frequency(GHz) |
|---|---|---|---|
| TM010 | 1.275009E+01 | TE011 | 2.195589E+01 |
| TE111 | 1.282993E+01 | TM111 | 2.195589E+01 |
| TM011 | 1.522870E+01 | TE212 | 2.322788E+01 |
| TE211 | 1.820685E+01 | TE311 | 2.377754E+01 |
| TE112 | 1.930420E+01 | TE012 | 2.626987E+01 |
| TM110 | 2.031533E+01 | TM112 | 2.626987E+01 |
| TM012 | 2.097519E+01 | TE113 | 2.682152E+01 |

FIGURE 2.4: Resonant Frequencies in cavity of 18mm diameter and 18mm height

From the resonant frequencies it can be seen that, TE011 and TM111 modes are degenerate. This degeneracy can be removed by modifying the shape of the resonator slightly. In our case, the mode splitting is archived by cutting small grooves at the top and bottom of the cavity. The net effect is that TM mode sees an effectively larger cavity, thus shifting it's resonant frequencies lower from the TE mode.

[1] Appendix-1

## 2.5 Cavity design for ESR

ESR experiments needs an oscillating field at microwave frequencies. Ordinary circuit elements can not be used at high frequencies because the skin effect creates a high resistance and energy will be lost in the form of radiation. Cavities provide a solution to overcome this issue[8].

For spin resonance experiments, TE011 mode is has a few interesting properties which makes it an ideal candidate. The magnetic field is maximum at the center of the cavity, which provides an ideal place to insert the sample. Moreover, the theoretical quality factor of this mode is four times larger than other modes.

The electric and magnetic fields in TE011 mode are given below.

$$E_r = 0 \tag{2.15}$$

$$E_\theta = -\sqrt{\frac{\mu}{\epsilon}} J_0^{'}(\frac{2x_{01}}{d}) sin(\frac{\pi}{h}z) \tag{2.16}$$

$$E_z = 0 \tag{2.17}$$

$$H_r = \frac{\frac{\pi}{h}}{\sqrt{\frac{2x_{01}}{d}^2 + \frac{\pi}{h}^2}} J_0^{'}(\frac{2x_{01}}{d}r) cos(\frac{\pi}{h}z) \tag{2.18}$$

$$H_\theta = 0 \tag{2.19}$$

$$H_z = \frac{\frac{2x_{01}}{h}}{\sqrt{\frac{2x_{01}}{d}^2 + \frac{\pi}{h}^2}} J_0(\frac{2x_{01}}{d}r) sin(\frac{\pi}{h}z) \tag{2.20}$$

where h is the height of the cavity

d is the diameter of the cavity

$J_0(x)$ is the Bessel's function of order zero

$J_0^{'}(x)$is the derivative of $J_0(x)$

$x_{01}$ is the first zero of $J_0(x)$

## 2.6 Surface Plots of TE011 mode

The field distribution of $H_r$ and $H_z$ shows the following pattern.

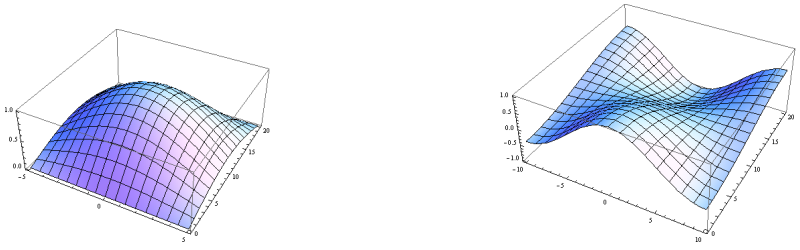

(A) $H_z$ in TE011 mode

(B) $H_r$ in TE011 mode

FIGURE 2.5: Surface plots of TE011 Mode

## 2.7 Simulation

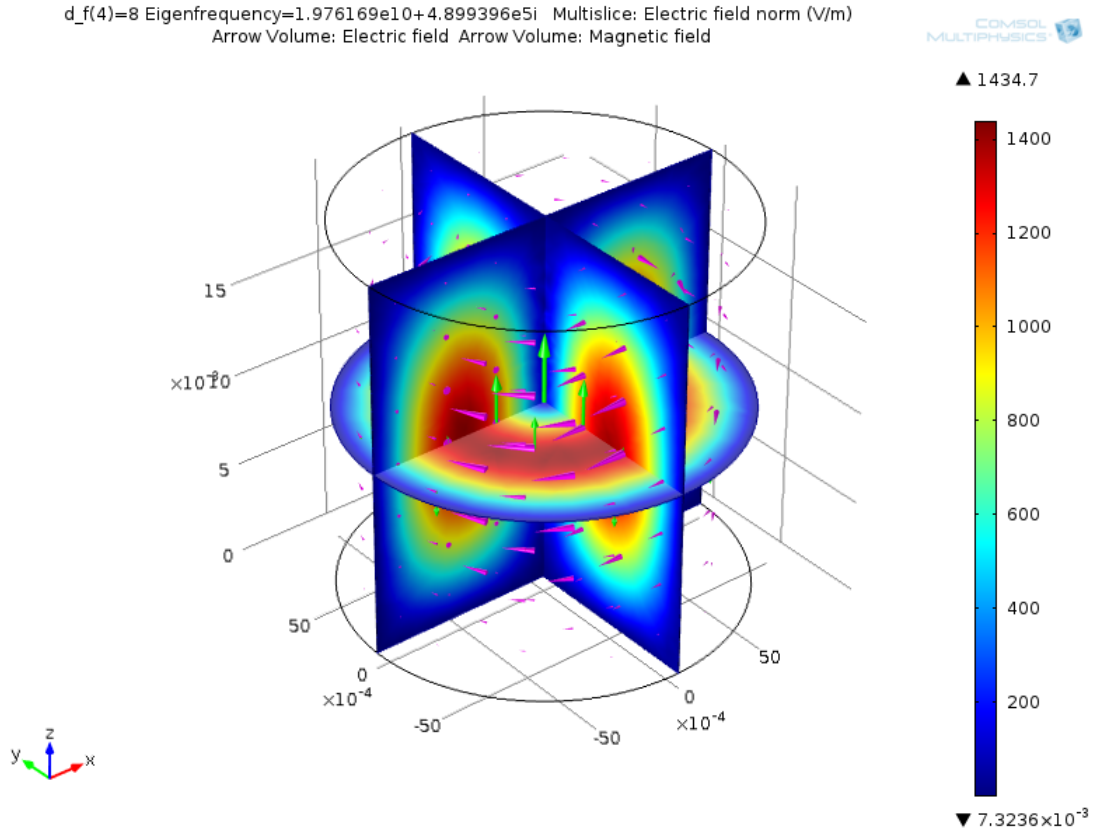


FIGURE 2.6: Simulation of TE011 Mode

A simulation is performed to visualize the fields inside the cavity. This figure shows the electric field of TE011 mode inside the cavity. One can infer from the simulation that the electric field is reaches a minimum value at the center. The magnetic field and electric field directions are also shown in the figure.

## 2.8 Q-factor for the cavity

Quality factor (Q-value) is an essential parameter for estimating the quality of cavity resonators. The high Q-value indicates the high accuracy and the narrow bandwidth of the cavity resonator. Q-factor is a measure of strength of damping near resonant frequency. There are actually two different common definitions of the Q factor of a resonator:

**Definition via energy storage:** Q factor is $2\pi$ times the ratio of the stored energy to the energy dissipated per oscillation cycle, or equivalently the ratio of the stored energy to the energy dissipated per radian of the oscillation. For a microwave or optical resonator, one oscillation cycle is understood as corresponding to the field oscillation period, not the round-trip period.

$$Q = 2\pi \left( \frac{Stored\ energy\ per\ cycle}{Energy\ lost\ per\ cycle} \right) \tag{2.21}$$

**Definition via resonance bandwidth:** Q factor is the ratio of the resonance frequency and the full width at half-maximum (FWHM) bandwidth of the resonance.

$$Q = \frac{f}{\Gamma} \tag{2.22}$$

The spectrum of the transmitted power in the cavity is a Lorentzian with two parameters

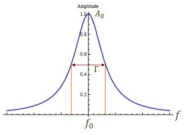

FIGURE 2.7: Q- factor: Spectrum of the transmitted power

namely FWHM and Center frequency.

$$A(f) = \frac{A_0}{(f - f_0)^2 + (\Gamma)^2} \tag{2.23}$$

Surface roughness has a big effect on metal loss. When the roughness of the cavity is of the orders of the skin depth of the conductor, the attenuation will increase. Surface roughness can be quantified by using RMS roughness. This will decrease the quality factor.

The quality factor of the cavity resonator can be improved by plating the walls of the cavity with silver. This decreases the electric losses. For copper cavities, plating with silver or gold will decrease the oxidization and improve the quality factor.

(A) Cavity with grooves

(B) Cavity with loop antenna

FIGURE 2.8: Cavity Resonator

## 2.9 Cavity Measurements using VNA

A copper cavity with the same dimensions is manufactured, and grooves were made inside the cavity to ensure the elimination of degeneracy. Two loop antennas, as shown in figure, are used to feed the microwave energy into the cavity. An SMA connector is soldered into one end of the loop antenna as shown in figure.

VNA calibration is performed and a two-port microwave S-parameter ($S_{12}$) is measured. The observed resonance spectrum is shown below. Quality factor is calculated by fitting the observed spectrum to a Lorentzian function.

The unloaded quality factor is calculated to be 11509 at the resonance.

## 2.10 Electron Spin Resonance using cavities

In the experiment, the spin transitions are obtained by sweeping the magnetic field continuously using an external magnetic field. The Vector network analyzer is used to excite the cavity with a microwave signal and the absorption spectrum is observed in the network analyzer. This setup is shown in the figure. The sample ($NH_4CuPO_4.H_20$), a spin 1/2 Heisenberg dimer, is then inserted into the cavity. The magnetic field is swept around the predicted value, and changes in the peak position of the TE011 mode in the cavity are measured and plotted against the magnetic field. This graph signifies an absorption in the energy, implying a spin resonance phenomenon.

FIGURE 2.9: Q- factor of cavity at TE-011 Mode

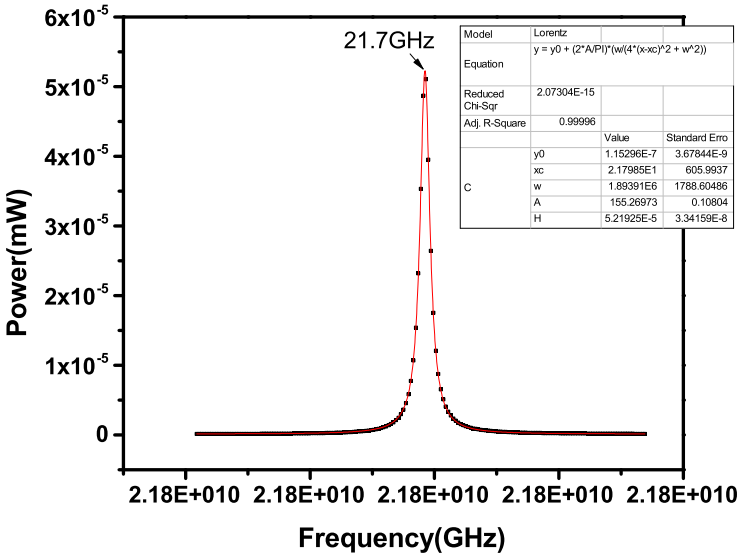


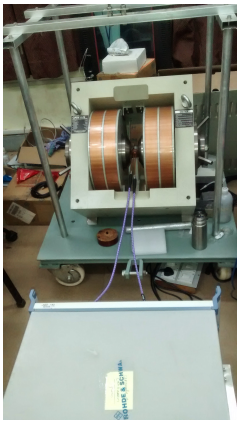

FIGURE 2.10: Setup for ESR

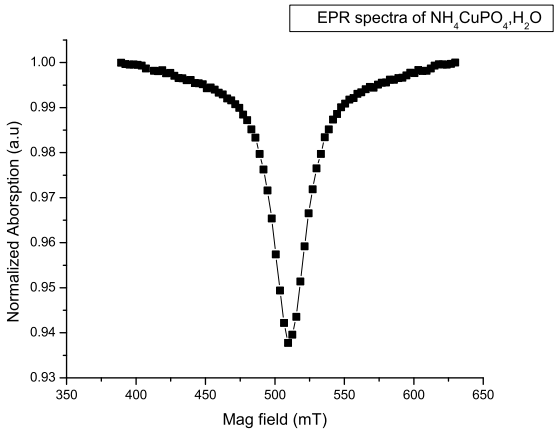


FIGURE 2.11: Observed absorption using cavity resonator

# Chapter 3

# Microstrip Resonators

## 3.1 Microstrip Basics

The general structure of a Microstrip line is shown in figure. It consists of a dielectric substrate sandwiched between two conducting layers. The conducting strip is on the top of the dielectric with a width(W) and thickness (t), where as the bottom conducting layer acts as a ground plane.

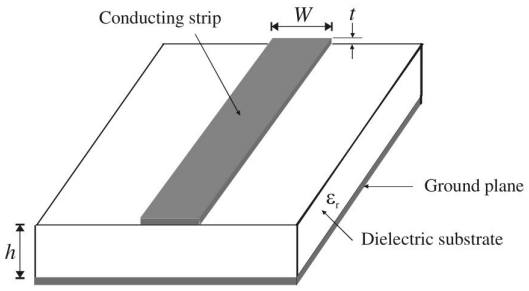


FIGURE 3.1: A general Microstrip line

The increasing necessity for high frequency antennas, filters, and oscillators demanded engineers to come up with new ideas. Microstrip planar circuits can be etched on an dielectric substrate, with cheap lithographic techniques, and provides a canvas for designers to precisely control their operation in the microwave regime.

### 3.1.1 Propagation in Microstrips

The electromagnetic fields in microstrip are called quasi-TEM modes. The fields extend within two media- air and dielctric substrate. Because of this reason, a microstrip can not support a pure TEM wave. In a pure TEM mode, the wave has only transverse

components. When two media are present, the waves in Microstrip will consist of a longitudinal component. Moreover, the propagation velocities of the wave will not only depend on the material properties, but also on the physical dimension of the strip. Using these parameters, one can design a microstrip resonator or filter which resonates at a desired frequency.

When the longitudinal components are very small when compared to transverse components, they can be neglected and the transmission lines behaves approximately same as that of TEM mode of a co-axial cable. This is called quasi-TEM approximation [9].

### 3.1.2 Effective Dielectric Constant and Characteristic Impedance

In the microstrip circuits, the transmission line can be described by using two parameters, the characteristic impedance ($Z_C$) and effective dielectric constant($\epsilon_r$). Although theoretical approximations exist for calculation, it is desirable to perform an electromagnetic simulation to optimize the structure. The closed form expressions for the evaluation of parameters is given below.

### 3.1.3 Characteristic Impedance ($Z_C$)

The characteristic impedance is given as follows [9].

For $\frac{W}{h} \leq 1$:

$$Z_c = \frac{\eta}{2\pi\sqrt{\epsilon_r}} ln\left(\frac{8h}{W} + 0.25\frac{W}{h}\right) \tag{3.1}$$

### 3.1.4 Effective Dielectric Constant

The effective dielctric constant is given as follows [9] .

For $\frac{W}{h} \leq 1$:

$$\epsilon_{reff} = \frac{\epsilon_r + 1}{2} + \frac{\epsilon_r - 1}{2}\{(1 + 12\frac{h}{W})^{-0.5} + 0.04(1 - \frac{W}{h})^2\} \tag{3.2}$$

## 3.2 Microstrip Resonators

A planar microstrip resonator contains at least one resonant electromagnetic field. Microstrip resonators form basic building blocks of filters, oscillators and various tuned amplifiers.

In literature, various designs have been proposed for detecting electron spin resonance using planar resonators. This thesis adapts a open loop-gap resonator structure as described here[10]. The resonance frequency typically occurs when the electric and magnetic stored energies cancel and only real power is dissipated.

## 3.3 Quality factor and Loss

The unloaded quality factor of any resonator is given by

$$Q_u = \omega \left( \frac{\text{Time-average energy stored in resonator}}{\text{Average power lost in resonator}} \right) \tag{3.3}$$

Losses in microstrip resonators occurs mainly due to three mechanisms conductor, dielectric, and radiation. The total unloaded quality factor is determined by using this equation.

$$\frac{1}{Q_u} = \frac{1}{Q_c} + \frac{1}{Q_d} + \frac{1}{Q_r} \tag{3.4}$$

where $Q_c$, $Q_d$ and $Q_r$ are conductor, dielectric and radiation quality factors respectively. To fully evaluate the performance of a resonator, calculations are usually performed using simulation software. Nevertheless, one can use the following equations to get an approximation.

The Quality factor of conductor is given by

$$Q_c = \frac{\pi}{\alpha_c \lambda_g} \tag{3.5}$$

where $\alpha_c$ is the conductor attenuation constant and $\lambda_g$ is the guided wavelength of the microstrip line

The dielectric loss is calculated by using

$$Q_d = \frac{1}{tan\delta} \tag{3.6}$$

where $\delta$ is the tangent loss of the dielectric.

The calculation of radiation Q is not trivial. Radiation losses occurs from numerous reasons including shape of resonator, dielectric material, thickness of substrate and

discontinuities. Generally, microstrip resonators are enclosed with conducting housing walls. The other loss loss mechanisms can be estimated using expressions, but a full electromagnetic simulation must be performed to analyze the radiation losses [9].

It is given as

$$Q_r = \omega \left( \frac{\text{Time-average energy stored in resonator}}{\text{Average power lost in housing walls}} \right) \tag{3.7}$$

## 3.4 Feeding methods

To match the input impedance of the resonator to 50Ω, a feeding method must be employed. Planar resonators are generally fed by using coaxial or microstrip feed. A feedline is used to excite or radiate by direct or indirect contact [11].

In this thesis, we fed the resonator using a Microstrip line feed.

### 3.4.1 Microstrip line feed:

A 50Ω microstrip transmission line is used to feed the resonator. Microstrip line feed is one of the easy to fabricate as it is a just conducting strip connecting to the resonator. It is simple to model and easy to match by controlling the inset position. However the disadvantage of this method is that the losses in this method are high.

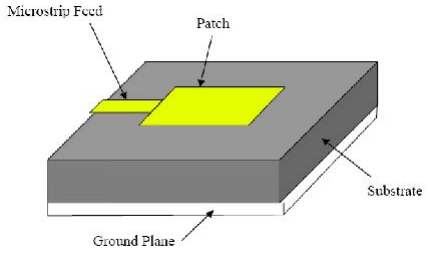


FIGURE 3.2: Microstrip Line feed

### 3.4.2 Coaxial feed

In this method of feeding, the inner conductor of coaxial cable is attached to the resonator directly by drilling a hole through the substrate and outer conductor is grounded to the base conductor of the resonator. This method of feeding is easier to match, but difficult to model, especially for thick substrates.

# Chapter 4

# Planar Resonator: Design and Simulation

## 4.1 Design of Resonator

Traditional cavities like the one described in the previous chapter operate in transverse electric mode for the the generation oscillating magnetic field. Microstrip resonators operate in TEM mode and the resonance frequency is dictated by the dimensions of the patch and the effective relative permittivity of the medium. Much similar to cavities, in microstrip resonators, one can have a mode in which the magnetic field will be maximum at center. This will be especially useful in low temperature measurements because the volume of the resonator becomes low. This chapter summarizes the design and simulation of planar resonator for electron spin resonance(ESR) experiments. In this thesis, a gap coupled rectangular patch resonator has been designed [10].

### 4.1.1 Substrate Details

A Rogers Duroid 5870 substrate is used to fabricate the microstrip resonator. RT/duroid 5870 laminates have the lowest electrical loss of any reinforced PTFE material, low moisture absorption, are isotropic, and have uniform electrical properties over frequency. The parameters used in simulation are given in the table below.

| Property | Value(units) |
|---|---|
| Thickness of dielectric | 787(microns) |
| Dissipation factor | 0.0012 |
| Copper Layer thickness( top and bottom) | 35(microns) |
| Dielectric constant | 2.33 |

### 4.1.2 Resonator Details

The planar resonator consists of a strip conductor of width w, length l on a substrate of thickness h and relative permittivity $\epsilon_r$, with a copper layer of thickness t as shown in the figure. The details of the structure are given below.

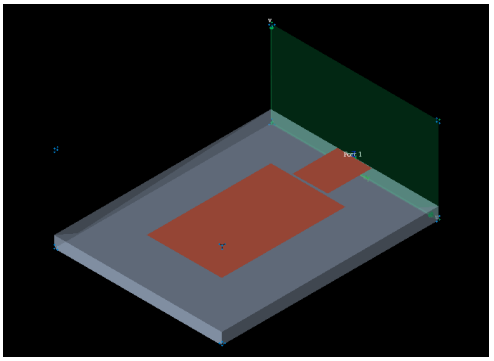

FIGURE 4.1: Microstrip Resonator

| Property | Value(units) |
|---|---|
| Width of the resonator(w) | 5(mm) |
| Length of the resonator(l) | 8.3 (mm) |
| Resonator gap(g) | 150 (microns) |
| Height of substrate(h) | 787 (microns) |
| Thickness of copper layer(t) | 35 (microns) |

## 4.2 Resonant frequencies

As described in the previous chapter, the resonant modes in this microstrip resonator can be approximated as a quasi-TEM mode and the resonant frequency $f_0$ is given by

$$f_0 = \frac{nc_0}{2(l + \Delta l)\sqrt{\epsilon_{reff}}} \tag{4.1}$$

where $c_0$ is the speed of light, n is the axial mode index, and $\Delta$l is the correction due to fringe electric field at the end of the resonator.

This fundamental mode has an interesting field pattern that will be useful for ESR experiments, the electric field at the resonant frequency at the center of the strip attains a minimum value where as the magnetic field attains a maximum value. This provides a way to interact with the magnetic sample. The idea is to place the sample near center of the strip and apply a external magnetic field perpendicular to this field, and observe electron spin resonance. To archive that, the resonator must have a resonant frequency in the X-band (7-11.2 GHz.) and the design must be done in such a way that the reflection coefficient at the resonance frequency will be minimum.

The presence of a small gap between the resonator and feedline complicates the analysis. Although some theoretical expressions were proposed, it is better to perform a full electromagnetic simulation to optimize the resonant frequencies.

## 4.3 Design of the microstrip feed

To match the input impedance of 50Ω, one has to calculate the width and length of the microstrip feed. In any real device, it is quite difficult to obtain impedance matching at a broadband range. For all general purposes, a return loss less than 10dB which corresponds to a VSWR of 1-2 is considered as acceptable impedance matching.

The design elements are generally constructed using quarter wave($\lambda/4$) elements. In this case, for a frequency of 11GHz., the corresponding $\lambda/4$ value is 6.8 mm.

LineCalc( Agilent Inc.)[12] has been used to calculate the width for Rogers 5870 substrate. For a $\lambda/4$ element resonator, the width of the feedline for a 50Ω match are given below. It can be observed from the table that the width of the resonator plays an important role in controlling the impedance.

| Width | Length | Impedance |
|---|---|---|
| 2.318910 | 4.818540 | 50.00000 |
| 2.500 | 4.18 | 47.590100 |
| 1.162770 | 4.93 | 75.00000 |

## 4.4 Simulation of proposed design

Advanced Design System (ADS) [13] is an electronic design automation software for RF, microwave, and high speed digital applications. It supports schematic design as well as layout design. ADS uses method of moments (MoM) for the simulation of planar

structure, this is a faster method when compared to other frequency domain methods like FEM. The design process in Agilent ADS follows a simple hierarchy.

- **Creating a schematic**:
- **Generating the layout**
- **Define substrate parameters**
- **Meshing the design and simulation**
- **Obtaining the S-parameters**

### 4.4.1 Schematic Design

The substrate is defined as a schematic with the values described above. The schematic design flow is shown in the figure below.

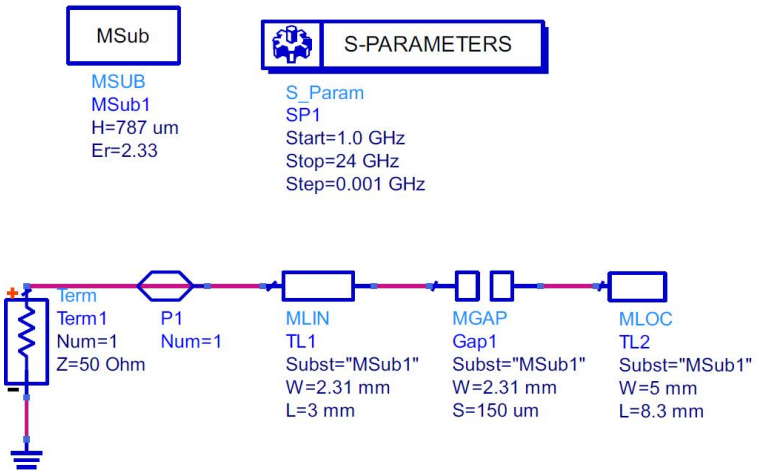


FIGURE 4.2: Schematic Design in ADS

### 4.4.2 Layout Generation and Meshing

The schematic could be directly generated as a layout on the substrate. A broadband simulation of 1-24 GHz. is performed initially, and after finding the resonant frequency,

a finer simulation was performed around the resonance. The following figure shows the meshed layout design in ADS.

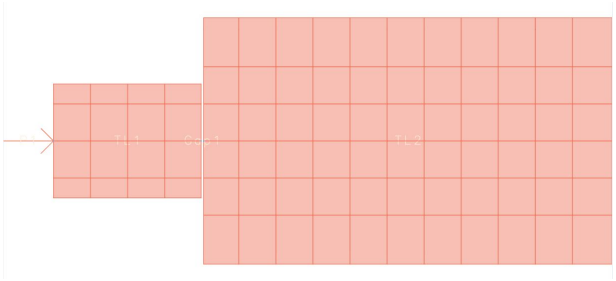

FIGURE 4.3: Meshed layout generated in ADS

### 4.4.3 Effect of gap on $S_{11}$

The width of the resonator patch is varied to control the quality factor, where as the length is varied to control the resonant frequency. The gap(g) between the feedline and the resonator specifies the coupling.

Simulations are performed using various design parameters. The gap between the resonator and the feedline controls the coupling. The gap is varied between 35$\mu$m to 150$\mu$m. It is observed that for the 35$\mu$m gap, the return loss($S_{11}$) is minimum implying maximum energy transfer. Although 35$\mu$m coupling gap gives us the ideal results, the minimum resolution of our PCB fabrication is 150$\mu$m. Hence, the design has been changed to 150$\mu$m. A graph showing the variation of $S_{11}$ with change in gap is shown below.

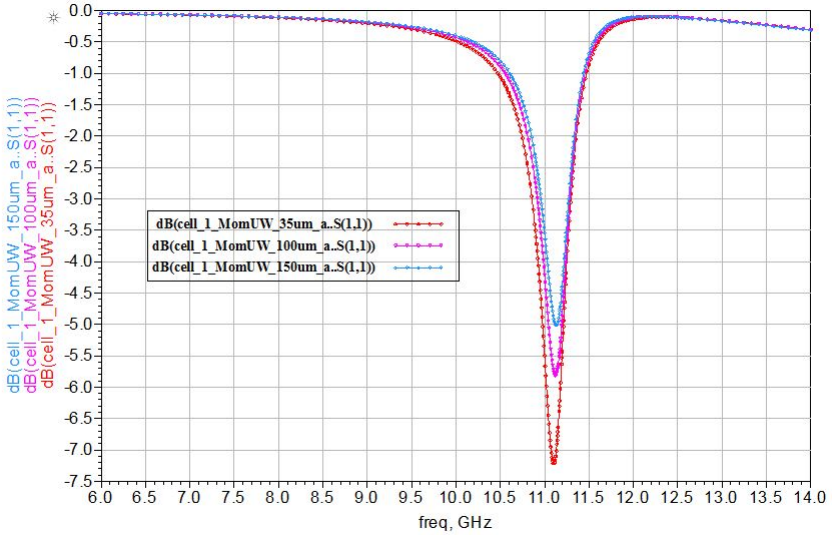


FIGURE 4.4: Simulated Gap vs $S_{11}$: The return loss is minimum for least gap

### 4.4.4 Resonant Frequencies and Quality factor

For the 150 micron gap, and resonator width of 5 mm and length of 8.3 mm, the resonant frequency is observed at 11.13 GHz.

The unloaded quality factor is determined by using the expression

$$Q_0 = \frac{(1+K)f_0}{\delta f} \tag{4.2}$$

In this expression, K denotes the coupling coefficient and $\delta f$ denotes the curve width where $\mid \Gamma \mid = \frac{(1+K^2)^{\frac{1}{2}}}{1+K}$ and $f_0$ denotes the resonant frequency.

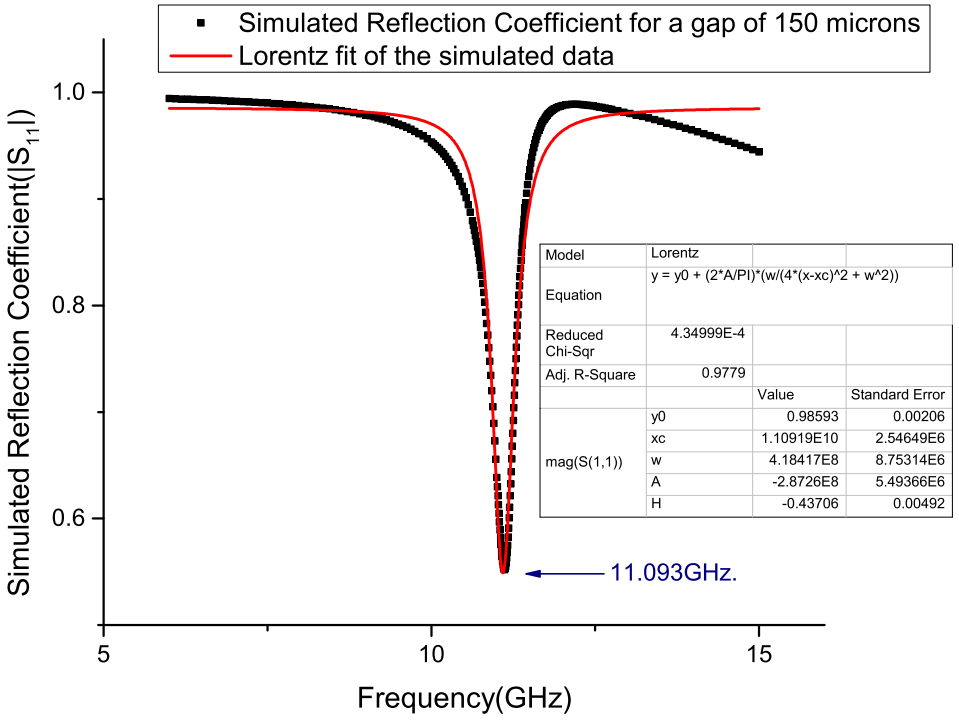


FIGURE 4.5: $S_{11}$: Simulated Resonant frequency and it's Lorentz fit

For an under-coupled system the value of K is given by

$$K = \frac{1- \mid \Gamma \mid (f_0)}{1+ \mid \Gamma \mid (f_0)} \tag{4.3}$$

And for an over-coupled system the value of K is given by

$$K = \frac{1+ \mid \Gamma \mid (f_0)}{1- \mid \Gamma \mid (f_0)} \tag{4.4}$$

The calculated unloaded Q-factor for the proposed structure is 30.

## 4.5 3D-FEM Simulation of proposed resonator

After optimizing the design in Agilent ADS, a full three dimensional electromagnetic FEM simulation is done. This simulation will allow us to see the electromagnetic field pattern on the microstrip resonator.

The proposed resonator including the substrate and the patch were drawn in Keysight EMPro [14] .

There are some advantages in using this software instead of Ansys HFSS, frequently used in academic community. EMPro has both Finite element method(FEM) and finite difference time domain(FDTD) engines. Depending upon the problem, one can choose a method which converges faster. For example, if one wants to work on a structure resonant at a very high frequencies, a time domain simulation will be able to find the resonances easily when compared to frequency domain methods like finite element method.

For the simulation in this thesis, we know the approximate resonant frequency beforehand. Hence, it is easy to do a finite element method simulation. The simulated $S_{11}$ response in FEM is shown in the figure below.

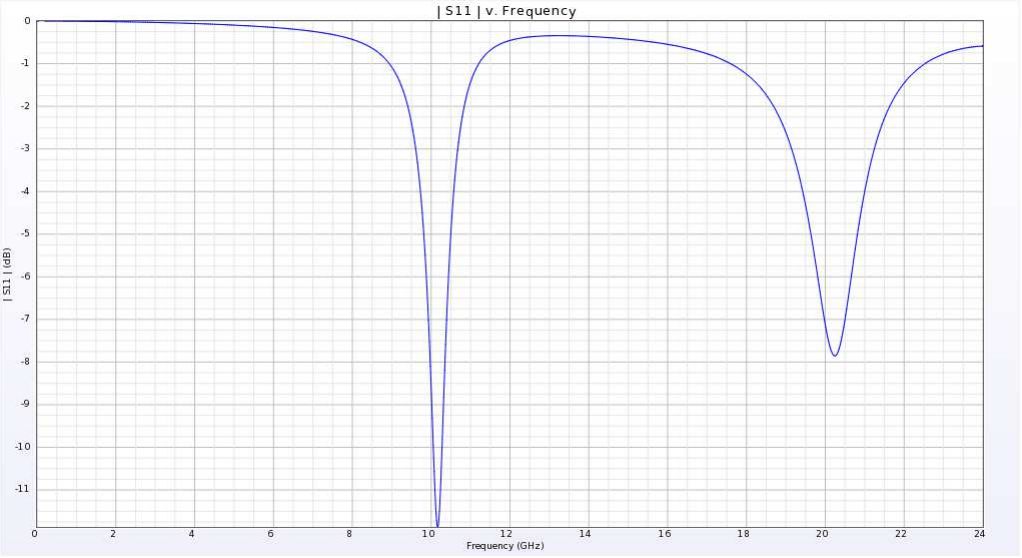


FIGURE 4.6: Simulated $S_{11}$ using Keysight

The simulated electric and magnetic field patterns at the resonance frequency are shown in the figure.

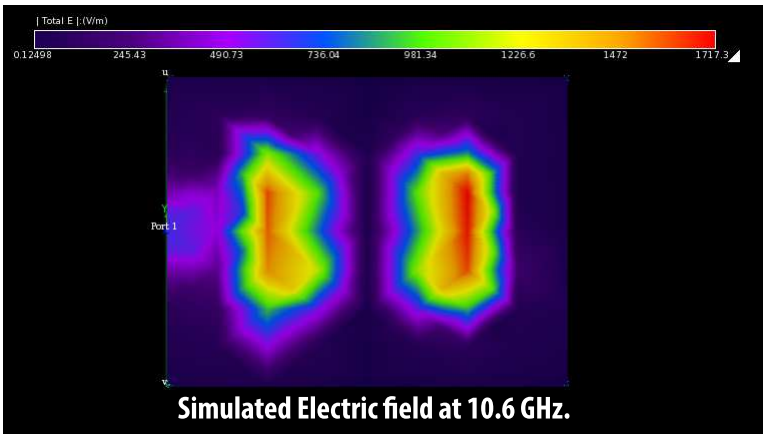


FIGURE 4.7: Electric field on the microstrip

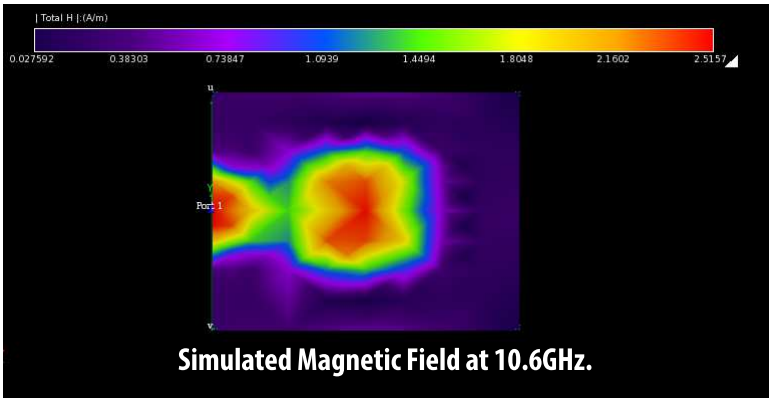


FIGURE 4.8: Magnetic field on the microstrip

The simulation clearly shows that the electric field at the center of the strip is minimum and where as the magnetic field intensity reaches a maximum value 2.51 A/m at the center of the strip. Just like the cavity, the proposed resonator provides a way to generate oscillating microwave magnetic field at higher frequencies. The downside of having a microstrip resonator instead of a cavity is that the quality factor is quite low.

# Chapter 5

# Fabrication and Measurement

## 5.1 Fabrication of the resonator

This section describes the fabrication of the simulated microstrip resonator proposed in the previous chapter. Optical lithography is used to fabricate the resonator on the substrate.

The following steps explains the photo lithographic process adapted in making the pattern.

- Initially, it is crucial to make the computer aided design (CAD) of the pattern. The negative of this design printed on a transparent sheet is used as a mask.

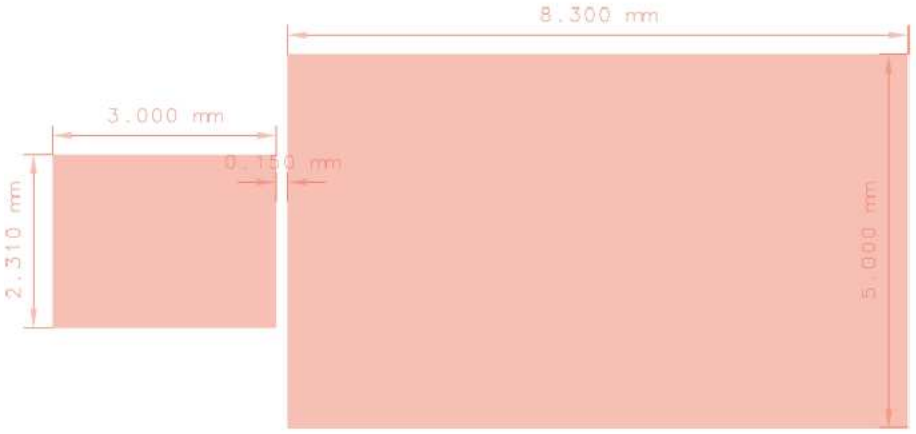


FIGURE 5.1: CAD Design

- A double sided copper clad substrate RT5870 with dimensions 25 mm X 25 mm is thoroughly cleaned using acetone and dried. Dust particles or impurities present

on the copper clad surface introduce discontinuity in the etched pattern that alters the resonant frequency.

- In the next step, a negative photo-resist film is laminated to the cleaned and dried copper clad substrate. The negative mask prepared in the first step is firmly placed on the photo-resist laminated copper clad substrate. The masked and photo-resist laminated copper clad substrate is exposed to ultra violet (UV) light.

- The next step is to develop the UV exposed photo-resist laminated copper clad substrate. The photo-resist exposed to UV light becomes hard and dark blue in colour while unexposed photo-resist remains light blue and dissolves in the developer solution. Sodium Carbonate is used as the developer.

- Finally, the developed copper clad substrate is chemically etched by Ferric Chloride $FeCl_3$ solution. The copper parts except underneath the hardened photo resist dissolve in $FeCl_3$. The etched substrate is rinsed in running water to remove any etchant and then dried. The hardened photo-resist is removed using Sodium Hydroxide. The photo-lithographically fabricated rectangular microstrip patch resonator is shown in figure.

FIGURE 5.2: Fabricated Microstrip using lithography

## 5.2 Microstrip Housing

To provide support for connecting the SMA connector, a ground base made up of Copper or Aluminum is used. Holes are drilled carefully into the substrate and tightly screwed to maintain good contact. The microstrip resonator with the housing is shown below.

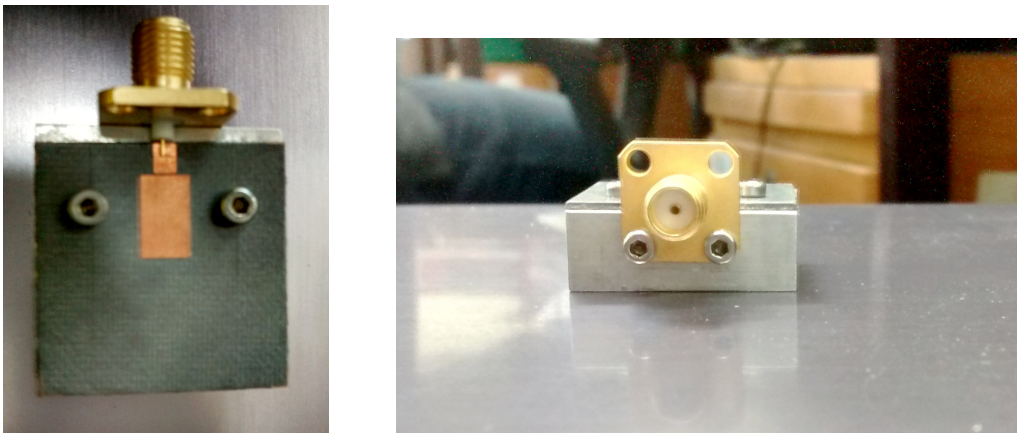

(A) Top view (B) Side view

FIGURE 5.3: Microstrip Resonator with housing

## 5.3 Connecting the terminal connector

After ensuring proper grounding, the launchers of SMA connector are soldered into the microstrip line. The soldering must be done carefully, and the position of the launcher needs to be symmetrical. After soldering, the continuity of the circuit is tested using a multimeter. The fabricated microstrip resonator is shown below.

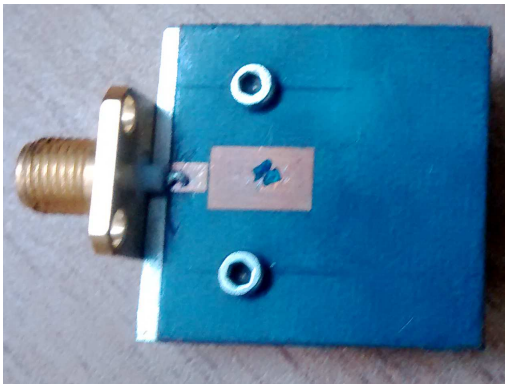

FIGURE 5.4: Soldered Microstrip resonator

## 5.4 Measurement using Vector Network Analyzer

Before doing any measurement, the VNA must be calibrated. This eliminates the errors in measurement due to losses in the coaxial cable. The calibration is done by using a calibration kit. It consists of a standard short (S), match (M) and open (O).

The measured $S_{11}$ from the VNA at the resonance frequency is shown below. This signifies that the return loss is minimum at resonant frequency($f_0$) and hence the input

microwave energy is transferred into the resonator. Ideally, the design with a gap of 35 microns would have improved the performance of the resonator, but our photolithographic has the minimum possible resolution of 150 microns. The simulated and

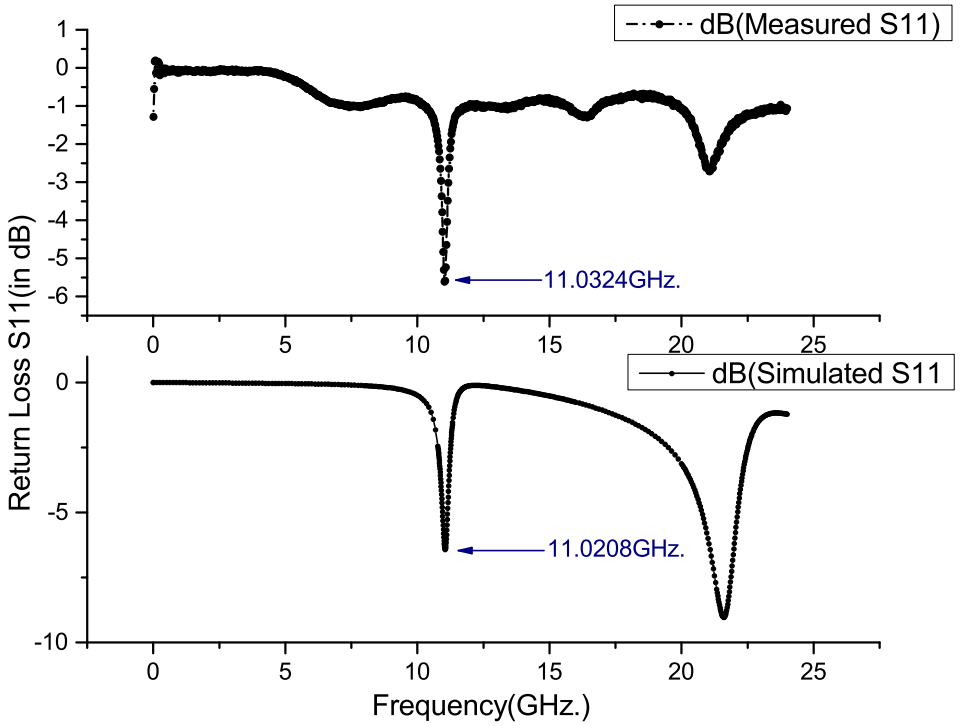


FIGURE 5.5: Measured vs Simulated $S_{11}$

measured $S_{11}$ values show a close match. The reflection coefficient and it's fit to a Lorentzian fit is shown in the figure below.

## 5.5 Quality factor from measured $\Gamma$

Q-factor is determined from the obtained Lorentz fit of the measured reflection coefficient, using

$$Q = \frac{f_c}{\text{Full width at half maximum}} \tag{5.1}$$

This fit gives a quality factor of about *38.405*. There is a discrepancy betwen simulated and measured quality factors. It could be due to the sensitive nature of the measurement from the vector network analyser.

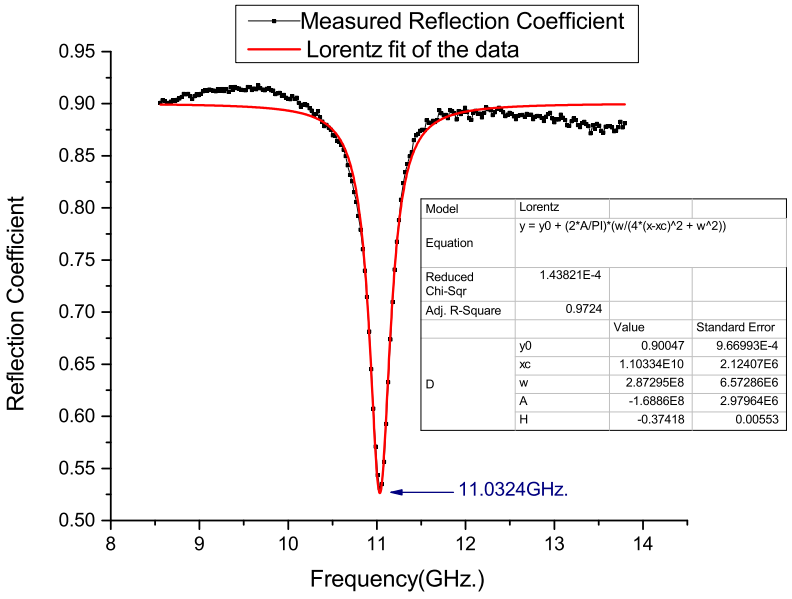


FIGURE 5.6: Lorentz fit to the measured Reflection Coefficient

# Chapter 6

# Conclusion

We started with the aim of improving the sensitivity of spin resonance experiments. The road to improve the sensitivity has two paths, one is to improve the quality factor and the other one is to improve the filling factor. Conventional spectrometers use cavity resonators.

In cavity resonators, we tried to improve the quality factor. We have designed different sizes of cavities and observed that when the diameter to height ratio of cavity is close to one, the quality factor is maximum. We worked in TE011 mode because the theoretical quality factor of this mode is four times larger than any other mode. We were sucessful in designing a cavity with a quality factor of $\approx 10^5$. We have also obseved strong electron spin resonance signal from the cavity resonator.

Since cavities depends on the foramation of standing waves, the dimensions of cavity should be atleast $\lambda_{mw}^3$ where $\lambda_{mw}$ is the wavelength of the microwave. For samples with smaller number of spin, the sensitivity becomes low because the filling factor is very less. One easy suggestion would be to decrease the volume of the cavity, but doing this will increase the resonant frequencies.

The second path is to improve the filling factor, this improves the EPR sensitivity by using smaller microstrip resonators operating in fundamental TEM mode. A planar resonator for probing ESR in X-band has been designed. The proposed resonator is simulated and then fabricated. Although microstrip resonators have a very less quality factor, it is compensated by the higher filling factor.

Because of the limitations of the fabrication technique used in making the resonator, the minimum gap has to be changed to $150\mu m$ which effected the performance of the resonator. The measured return loss of 6 dB siginifies that only 55% of input power is being trasferred to the resonator.

The maximum return loss of 6 dB is not optimal for doing spin resonance experiments. It has been observed in literature that a return loss of 30 dB is essential for doing sensitive spin resonance experiements. Although the fabricated resonator showed poor performance when compared to cavities, an improved future design having lesser loop-gap(g) around 20-50 $\mu m$ will improve the performance of the resonator as described in the simulation part of the thesis. To improve the resolution, one suggestion would be to use focussed ion beam lithography or electron beam lithography.

This work has applications in various fields. The future of spin based quantum information processing relies heavily on improving the sensitivity of the resonator for smaller number of spins. Although microstrip resonators existed for decades, it is only recently researchers started using them as resonators for ESR experiements. Other high frequency phenomenon like Ferromagnetic resonance (FMR) require microstrip resonators. The field of spintronics aims to design new storage technologies by exploiting the properties of electrons like spin.

# Appendix A

# MATLAB Code for obtaining Resonant frequencies

This code can be used to generate the resonant frequencies. It takes in the radius and height of the cavity and the output gives all the resonant frequencies in GHz.

```
%function[freq,Q]=cavity(a,d,mu,epsilon)
a=input('Enter radius of cavity(mm)RADIUS!');
a=a*10^-3;
d=input('Enter height of cavity(mm)');
d=d*10^-3;
if a==0
    error('a can not be zero');
else if d==0
    error('d can not be zero');
    end
end
mu=8.85418782*10^-12;
epsilon=1.25663706*10^-6;
besselm=[2.405  5.52   8.654 11.792 14.931;
     3.832  7.016 10.173 13.324 16.471;
     5.136  8.417 11.62  14.796 17.960;
     6.38   9.761 13.015 16.224 19.409;
     7.588 11.065 14.373 17.616 20.827];

bessele=[3.832  7.016 10.173 13.324 16.471;
     1.841  5.332  8.537 11.701 14.863;
     3.054  6.706  9.969 13.17  16.347;
     4.201  8.015 11.345 14.585 17.788;
     5.317  9.282 12.681 15.964 19.196];
 aux1=sqrt(mu*epsilon);
for n=0:3
    for p=1:3
        for q=1:3
ke=sqrt((bessele(n+1,p)/a)^2+(q*pi/d)^2);
fresonante=ke/(2*pi*aux1);
fresonante=fresonante*10^-9;
```

```
fprintf('Resonant Frequency TE %d %d %d is %d GHz. \n\r',n,p,q,fresonante);

        end
    end
end
for n=0:3
    for p=1:3
        for q=0:3
km=sqrt((besselm(n+1,p)/a)^2+(q*pi/d)^2);
fresonantm=km/(2*pi*aux1);
fresonantm=fresonantm*10^-9;
fprintf('Resonant Frequency TM %d %d %d is %d GHz.\n\r ',n,p,q,fresonantm);
        end
    end
end
```

# Bibliography


[1] R Narkowicz, D Suter, and R Stonies. Planar microresonators for epr experiments. *Journal of Magnetic Resonance*, 175(2):275–284, 2005.

[2] Wikipedia. Electron paramagnetic resonance — Wikipedia, the free encyclopedia, 2004. URL http://en.wikipedia.org/wiki/Electron_paramagnetic_resonance.

[3] Rhode and Schwarz. Network analyzer. URL http://www.rohde-schwarz.com/en/products/test-measurement/network-analyzers/pg_overview_64043.html.

[4] Wikipedia. Return loss — Wikipedia, the free encyclopedia, 2004. URL http://en.wikipedia.org/wiki/Return_loss.

[5] Wikipedia. Standing wave ration — Wikipedia, the free encyclopedia, 2004. URL http://en.wikipedia.org/wiki/Standing_wave_ratio.

[6] Richard P Feynman, Robert B Leighton, and Matthew Sands. The feynman lectures on physics. vol. ii: Mainly electromagnetism and matter, 1964.

[7] Samuel Y Liao. *Microwave devices and circuits*, volume 3. Prentice Hall Englewood Cliffs, 1990.

[8] Anat Burger. *Optimization of a microwave resonator cavity to perform Electron Spin Resonance measurements on quantum dots*. PhD thesis, Massachusetts Institute of Technology, 2006.

[9] Jia-Shen G Hong and Michael J Lancaster. *Microstrip filters for RF/microwave applications*, volume 167. John Wiley & Sons, 2004.

[10] AC Torrezan, TP Mayer Alegre, and G Medeiros-Ribeiro. Microstrip resonators for electron paramagnetic resonance experiments. *Review of Scientific Instruments*, 80 (7):075111, 2009.

[11] Wiki. Feeding methods. URL http://microstrip-antennas.blogspot.in/2008/06/feeding-methods.html.

[12] Agilent. Agilent linecalc, . URL http://cp.literature.agilent.com/litweb/pdf/ads2008/linecalc/ads2008/Using_LineCalc.html.

[13] Agilent. Agilent ads, . URL http://www.keysight.com/en/pc-1297113/advanced-design-system-ads?cc=US&lc=eng.

[14] Keysight. Keysight empro. URL http://www.keysight.com/en/pc-1297143/empro-3d-em-simulation-software.